

# Evidence for a trigonal dimer of antibonding hydrogen in crystalline silicon

R. N. Pereira\* and B. Bech Nielsen

*Institute of Physics and Astronomy, University of Århus, DK-8000 Århus, Denmark*

(Received 29 December 2005; published 24 March 2006)

The infrared absorption spectra recorded on silicon crystals implanted with protons at cryogenic temperatures reveal three lines at 812, 1608, and 1791  $\text{cm}^{-1}$ , which originate from the excitation of local vibrational modes of a H defect. Measurements carried out on crystals subjected to uniaxial stress show that the 812  $\text{cm}^{-1}$  line results from excitation of a two-dimensional mode of a trigonal defect. Based on the analysis of the experimental data and on comparison with the properties of other known H defects in Si, we ascribe the 812 and 1791  $\text{cm}^{-1}$  lines to a wag mode and a stretch mode of a defect with one or more H atoms at antibonding sites and attached to neighboring Si atoms. A likely structure denoted  $\text{H}_2^{**}$  is proposed, where each one of two nearest neighboring Si atoms forms a bond with one H so that the two Si-H bonds point in opposite directions towards interstitial tetrahedral sites along the same  $\langle 111 \rangle$  axis.

DOI: [10.1103/PhysRevB.73.115208](https://doi.org/10.1103/PhysRevB.73.115208)

PACS number(s): 61.72.Ss, 61.72.Tt, 82.30.Rs, 78.55.Ap

## I. INTRODUCTION

Hydrogen plays a central role in a number of processes applied in semiconductor technology, and therefore its interaction with various semiconductor materials has been investigated intensively during the last decades.<sup>1-3</sup> Hydrogen atoms may be introduced unintentionally into semiconductors and normally compensate the prevailing doping by forming donor-H or acceptor-H complexes.<sup>4-7</sup> However, it may also be introduced intentionally as is the case for the passivation of dangling-bond states at Si/SiO<sub>2</sub> interfaces.<sup>2</sup> Consequently, detailed knowledge of the properties of H in semiconductors is essential to clarify the influence of this element on crystal growth, device processing, and operation stages. Proton implantation has been successfully used in combination with different spectroscopy techniques for thorough investigations of hydrogen defects in Si.<sup>8-13</sup>

When moderate doses of protons are implanted into Si at cryogenic temperatures (below 80 K), H atoms are present in their isolated forms, where the specific configuration depends on the position of the Fermi level in the crystal. In *p*-type material H is positively charged and at bond-centered sites ( $\text{H}_{\text{BC}}^+$ ). In *n*-type material negatively charged H at or close to the interstitial tetrahedral site is the energetically favorable configuration.<sup>9-11</sup> Light impurity atoms like H produce local vibrational modes (LVMs) with frequencies that are well above those of the crystal phonons. Therefore, infrared (IR) absorption spectroscopy is a powerful method for studies of H defects (see, for example, Refs. 12 and 13). Infrared absorption studies of Si implanted with protons at cryogenic temperatures revealed that the asymmetric stretch vibration of  $\text{H}_{\text{BC}}^+$  gives rise to an absorption line at 1998  $\text{cm}^{-1}$ .<sup>14</sup> The  $\text{H}_{\text{BC}}^+$  defects are thermally unstable above  $\sim 150$  K, where H becomes mobile. The diffusing H atoms interact with each other, forming  $\text{H}_2^*$  dimers,<sup>12</sup> and  $\text{H}_2$  molecules at interstitial tetrahedral sites.<sup>15-17</sup> The stability of these dihydrogen defects and their role for the diffusion of H in Si have been investigated previously both experimentally and theoretically.<sup>15-21</sup>

In this work, we report on a H defect in crystalline Si which we assign to a new H dimer of trigonal symmetry denoted  $\text{H}_2^{**}$ . The experimental evidence is obtained by *in*

*situ*-type IR absorption studies of proton-implanted Si crystals under uniaxial stress. The IR absorption data reveal three lines at 812, 1608, and 1791  $\text{cm}^{-1}$ , which originate from a trigonal defect. The 812  $\text{cm}^{-1}$  line is ascribed to the excitation of a twofold degenerate wag mode of H at an antibonding site ( $\text{H}_{\text{AB}}$ ), whereas the 1791  $\text{cm}^{-1}$  line represents the corresponding stretch mode. All the experimental data are consistent with the  $\text{H}_2^{**}$  dimer, which consists of two neighboring Si atoms each one bonded to a  $\text{H}_{\text{AB}}$ , so that the two equivalent Si- $\text{H}_{\text{AB}}$  units point in opposite directions along the same  $\langle 111 \rangle$  axis (see Fig. 1).

## II. EXPERIMENTAL DETAILS

Samples with dimensions of  $\sim 8 \times 8 \times 0.7$  mm<sup>3</sup> were cut from high-resistivity float-zone *n*-type Si crystals (P content  $\sim 4 \times 10^{13}$  cm<sup>-3</sup>), with less than  $5 \times 10^{15}$  cm<sup>-3</sup> of O and C, and were polished on the two opposing  $8 \times 8$  mm<sup>2</sup> faces. The samples were mounted in a cryostat, equipped with two CsI windows and one 100- $\mu\text{m}$ -thick Al window, through which the implantations were performed. The cryostat was placed inside a vacuum chamber which in turn was connected to the beam line of a tandem accelerator. The samples were implanted through one of the large faces with protons and/or deuterons with different energies in the range 5–10 MeV.

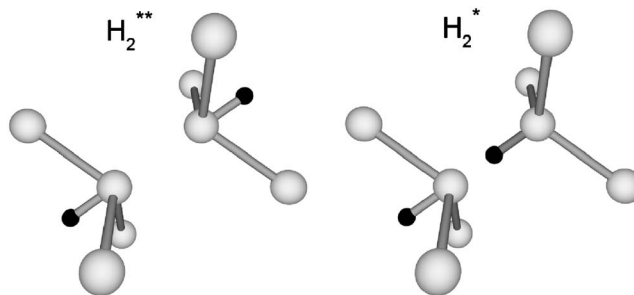


FIG. 1. Sketch with the structures of  $\text{H}_2^{**}$  and  $\text{H}_2^*$  in Si. Hydrogen and silicon atoms are represented by black and gray circles, respectively. In each defect, the two hydrogen atoms are located along the same  $\langle 111 \rangle$  axis.

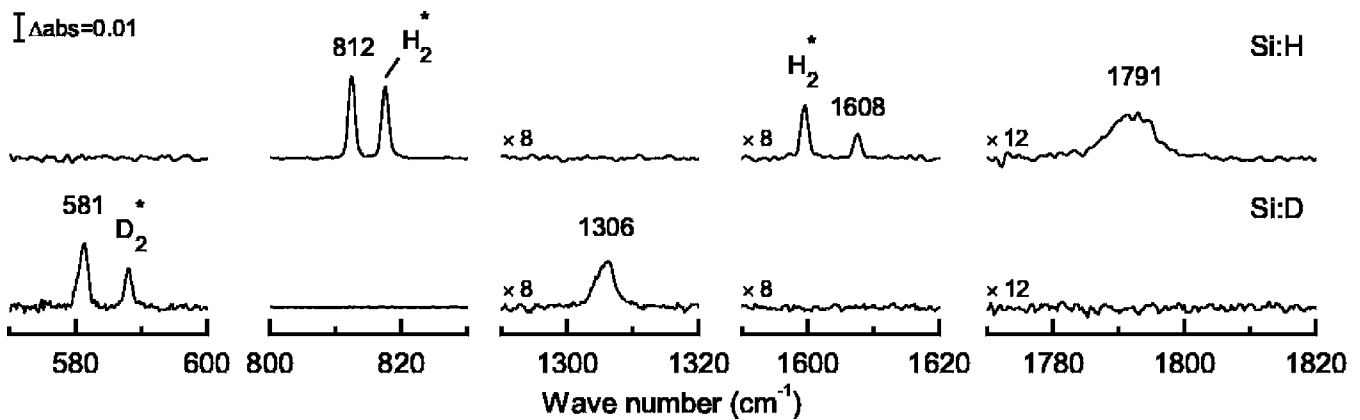


FIG. 2. Sections of absorbance spectra recorded on proton- (Si:H) or deuteron-implanted (Si:D) Si after annealing at 300 K.

The dose at each energy was adjusted to result in a uniform concentration of the implanted species of  $1-5 \times 10^{18} \text{ cm}^{-3}$  in the range  $150-550 \mu\text{m}$  below the surface. During the implantation the samples were kept at temperatures below 20 K using a closed-cycle helium cryocooler. After the implantation the cryostat was moved to a Nicolet System 800 Fourier-transform IR spectrometer, while keeping the samples temperature below 20 K. All spectra were recorded at  $\sim 8 \text{ K}$  with a spectral resolution of  $0.5 \text{ cm}^{-1}$ . Heat treatments of the samples were carried out *in situ* with a resistive heater connected to the sample holder and wired to a temperature controller, which allowed temperature stabilization within  $\pm 0.5 \text{ K}$ . Uniaxial stress measurements were performed on  $\sim 10 \times 2 \times 2 \text{ mm}^3$  samples with the smallest surfaces cut orthogonal to the [100], [110], or [111] direction, mounted in a helium-flow cryostat and using a homebuilt stress apparatus. In this case, the samples were implanted with protons at temperatures below 40 K and subsequently heat treated at 280 K for 30 min before the IR absorption was measured. Further details of the experimental setup and procedure are described elsewhere.<sup>22</sup>

### III. EXPERIMENTAL RESULTS

Figure 2 shows sections of the IR spectra obtained after low temperature implantation of Si with protons or deuterons and subsequent annealing for 30 min at 300 K. The spectrum

of proton-implanted Si displays sharp lines at 812 and  $1608 \text{ cm}^{-1}$ , together with a broader line at  $1791 \text{ cm}^{-1}$ . The three lines grow up together gradually upon heat treatments at temperatures in the range 50–300 K and they anneal out together after annealing at 320 K. Hence, they originate from the same defect. As shown in Fig. 2, the 812 and  $1791 \text{ cm}^{-1}$  lines shift down in frequency to 581 and  $1306 \text{ cm}^{-1}$ , respectively, when deuterons are implanted instead of protons. Hence, the ratios between the frequencies in the proton and deuteron case are 1.40 and 1.37. Both ratios are close to  $\sqrt{2}$ , which establishes that the lines originate from LVMs of H bound to a heavier element. To achieve information about the number of H atoms involved in the defect, IR spectra were recorded on samples implanted with overlapping profiles of protons and deuterons. No additional lines were observed in these spectra. Therefore, the defect either contains a single H or, if it contains additional H atoms, the dynamical interaction between the H atoms must be very small.

The effect of uniaxial stresses along the [100], [111], and [110] directions on the  $812 \text{ cm}^{-1}$  line is shown in Fig. 3 for IR light polarized parallel and perpendicular to the stress direction. Stress along the [100] direction splits the line into two components, only one of which is observed with light polarized parallel to the stress direction. Stress along the [111] direction splits the line into three components, only one of which is observed with light polarized parallel to the stress direction, whereas the other two are observed only

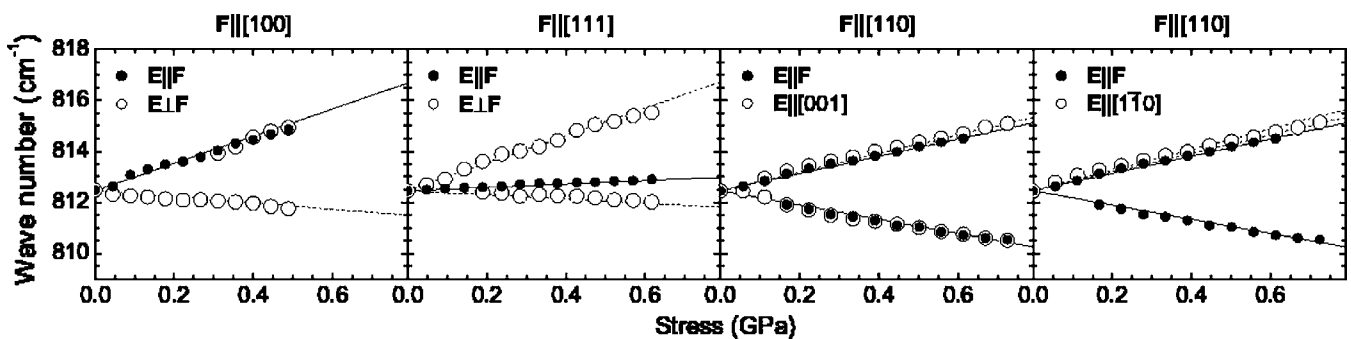


FIG. 3. Frequency shifts induced on the  $812 \text{ cm}^{-1}$  line by uniaxial stresses parallel to [100], [111], and [110] directions for the electric-field vector  $\mathbf{E}$  of the incident light ( $\bullet$ ) parallel and ( $\circ$ ) perpendicular to the stress direction  $\mathbf{F}$ . The solid (dotted) lines represent the best fit of the stress pattern for  $\mathbf{E}$  parallel (perpendicular) to  $\mathbf{F}$  of an  $A \rightarrow E$  transition of a trigonal defect.

TABLE I. LVM frequencies ( $\text{cm}^{-1}$ ) observed for the new lines in H- and D-implanted Si ( $\text{H}_2^*$ ), together with frequencies reported for  $\text{H}_2^*$  in Si.

$\text{H}_2^{**}$		$\text{H}_2^*$	
Mode	Freq.	Mode	Freq.
$E_u$ (Si- $\text{H}_{\text{AB}}$ wag)	812.4	$E$ (Si- $\text{H}_{\text{AB}}$ wag)	817.2
$E_u \otimes E_g$	1607.7	$E \otimes E$	1599.1
$A_{2u}$ (Si- $\text{H}_{\text{AB}}$ stretch)	1791.1	$A_1$ (Si- $\text{H}_{\text{AB}}$ stretch)	1838.3
$A_{1g}$ (Si- $\text{H}_{\text{AB}}$ stretch)	...	$A_1$ (Si- $\text{H}_{\text{BC}}$ stretch)	2061.5
$E_u$ (Si- $\text{D}_{\text{AB}}$ wag)	581.2	$E$ (Si- $\text{D}_{\text{AB}}$ wag)	587.7
$A_{2u}$ (Si- $\text{D}_{\text{AB}}$ stretch)	1306.4	$A_1$ (Si- $\text{D}_{\text{AB}}$ stretch)	1339.6
$A_{1g}$ (Si- $\text{D}_{\text{AB}}$ stretch)	...	$A_1$ (Si- $\text{D}_{\text{BC}}$ stretch)	1499.7

with light polarized perpendicular to the stress direction. This splitting pattern is characteristic for an  $A \rightarrow E$  transition of a trigonal defect.<sup>23</sup> The straight lines in Fig. 3 represent the best fit of the theoretical shifts to the data for such transition. Following the notation used in Refs. 22 and 23 the values of the parameters  $A_1$ ,  $A_2$ ,  $B$ , and  $C$  corresponding to the best fit are 2.06,  $-1.44$ ,  $-1.64$ , and  $1.77 \text{ cm}^{-1}/\text{GPa}$ , respectively. The fit is in very good agreement with the data for all stress directions and the relative intensities for the different light polarizations are also consistent with the theoretical values. Therefore, the  $812 \text{ cm}^{-1}$  line is assigned to a doubly degenerate LVM of a trigonal defect.

#### IV. DISCUSSION

The frequencies of H-related LVMs previously identified for  $\text{H}_2^*$  in Si are shown in Table I, together with those observed for our new lines. The  $\text{H}_2^*$  defect is formed by two neighboring Si atoms, one bonded to a  $\text{H}_{\text{AB}}$  and the other bonded to a H at a near bond-centered site ( $\text{H}_{\text{BC}}$ ), so that the two H and the two Si atoms are lying along the same  $\langle 111 \rangle$  axis (see Fig. 1).<sup>12</sup> As can be seen from the table, the frequencies of the  $812$ ,  $1608$ , and  $1791 \text{ cm}^{-1}$  lines are close to those of  $\text{H}_2^*$  at  $817$ ,  $1599$ , and  $1838 \text{ cm}^{-1}$ . The three latter lines are due to the doubly degenerate wag mode perpendicular to the Si- $\text{H}_{\text{AB}}$  bond, the first overtone of the wag mode, and the stretch mode along the Si- $\text{H}_{\text{AB}}$  bond, respectively.<sup>12,22</sup> Based on the similarities of the mode frequencies and on the symmetry deduced from our stress data for the  $812 \text{ cm}^{-1}$  mode, we conclude that the  $812$  and  $1791 \text{ cm}^{-1}$  lines are due to a twofold degenerate wag mode and a stretch mode associated with  $\text{H}_{\text{AB}}$  in a trigonal defect. The weak line at  $1608 \text{ cm}^{-1}$  we assign to an overtone of the  $812 \text{ cm}^{-1}$  mode or a combination mode. We shall discuss further the assignment of the latter line below. It is instructive to compare the frequency of the wag mode at  $812 \text{ cm}^{-1}$  with those of the wag mode of the donor-H defects in Si, where the H is also at an antibonding position attached to a Si atom along the  $\langle 111 \rangle$  axis containing the donor atom neighboring the Si atom.<sup>6</sup> These defects also have trigonal symmetry ( $C_{3v}$ ) and all display very similar frequencies for the doubly degenerate wag mode at  $\sim 810 \text{ cm}^{-1}$ .<sup>7</sup> These frequencies are again very

close to that of our  $812 \text{ cm}^{-1}$  line, which provides further support for our assignment. Moreover, the fact that the isotropic element of the piezospectroscopic tensor  $A_1 = 2.06 \text{ cm}^{-1}/\text{GPa}$  for the  $812 \text{ cm}^{-1}$  mode is similar to  $A_1 = 1.35 \text{ cm}^{-1}/\text{GPa}$ , reported for the  $817 \text{ cm}^{-1}$  mode of  $\text{H}_2^*$ ,<sup>12</sup> is also consistent with our assignment.

Based on the experimental findings, the defect giving rise to the  $812$ ,  $1608$ , and  $1791 \text{ cm}^{-1}$  lines has trigonal symmetry and contains at least one  $\text{H}_{\text{AB}}$  bonded to a Si atom. The obvious candidates are isolated H at an antibonding site, either neutral ( $\text{H}_{\text{AB}}^0$ ) or negatively charged ( $\text{H}_{\text{AB}}^-$ ). (The positive charge state is stable only at the bond-centered site.) The LVM frequencies of negatively charged  $\text{H}_{\text{AB}}$  attached to a Si atom (Si- $\text{H}_{\text{AB}}^-$ ) have recently been identified in Ge-rich SiGe alloys.<sup>24</sup> For a Si content of about 1 at. % the wag and stretch modes of Si- $\text{H}_{\text{AB}}^-$  are at  $816$  and  $1430 \text{ cm}^{-1}$ , respectively.<sup>24</sup> However, the stretch mode frequency decreases at a rate of  $-1.3 \text{ cm}^{-1}$  per at. % of Si up to a Si content of  $\sim 6$  at. %. If we extrapolate to obtain a frequency for pure Si, a stretch frequency of  $\sim 1300 \text{ cm}^{-1}$  is obtained for  $\text{H}_{\text{AB}}^-$ , in clear contradiction with that of our stretch mode at  $1791 \text{ cm}^{-1}$ . In addition, the stretch mode frequency of  $\text{H}_{\text{AB}}^-$  in pure Si which is obtained from *ab initio* theory is also low, i.e.,  $840 \text{ cm}^{-1}$ .<sup>25</sup> For  $\text{H}_{\text{AB}}^0$ , an even lower frequency associated with the vibration along the  $[111]$  axis is expected. Finally,  $\text{H}_{\text{AB}}^0$  and  $\text{H}_{\text{AB}}^-$  are found to be thermally unstable above  $250 \text{ K}$  from deep level transient spectroscopy data.<sup>11</sup> Thus we rule out the possibility that our lines originate from isolated  $\text{H}_{\text{AB}}^0$  or  $\text{H}_{\text{AB}}^-$ .

Alternatively, the lines could be due to a  $\text{H}_{\text{AB}}$  attached to one of the Si neighbors of a vacancy. We note that this structure would probably need to be positively charged ( $\text{VH}_{\text{AB}}^+$ ) to display trigonal symmetry. In the neutral or negatively charged states a Jahn-Teller distortion is expected to lower the symmetry to monoclinic I. However, we consider the  $\text{VH}_{\text{AB}}^+$  model unlikely, since it is not expected to be stable at  $300 \text{ K}$  against the formation of the vacancy-H defect, where the H is bonded inside the vacancy, for which the local deformation of the lattice is smaller. One may think of other trigonal structures which involve  $\text{H}_{\text{AB}}$  and intrinsic defects. However, these alternative structures should contain additional H atoms at different sites, for which we would expect to observe additional LVMs in our spectra. Therefore, we rule out such models.

All the experimental data are consistent with the  $\text{H}_2^{**}$  defect which contains two equivalent  $\text{H}_{\text{AB}}$  atoms each one attached to one of the Si atoms of a Si-Si bond, forming two Si- $\text{H}_{\text{AB}}$  units aligned in opposite directions along a  $\langle 111 \rangle$  axis (see Fig. 1). Within this model, the  $812 \text{ cm}^{-1}$  line is due to excitation of a doubly degenerate mode  $E_u$ , where the two H atoms vibrate in-phase perpendicular to the  $\langle 111 \rangle$  axis (wag), and the  $1791 \text{ cm}^{-1}$  line is due to a  $A_{2u}$  mode, where the two H atoms vibrate together in the same direction along the  $\langle 111 \rangle$  axis (stretch). The  $\text{H}_2^{**}$  has inversion symmetry ( $D_{3d}$  point group). Therefore, the gerade wag and stretch modes are IR inactive and thus not observed. These modes transform like the irreducible representations  $E_g$  and  $A_{1g}$  of  $D_{3d}$ . The overtones of the  $E_u$  mode are optically inactive,<sup>26</sup> and therefore the weak line at  $1608 \text{ cm}^{-1}$  cannot be an overtone

of the  $E_u$  mode. In the  $H_2^{**}$ , the two  $H_{AB}$  atoms will be only weakly coupled and, therefore, we expect the frequencies of the  $E_g$  and  $A_{1g}$  modes to be similar to those of the optically active modes  $E_u$  and  $A_{2u}$ , respectively. Due to anharmonicity, optical transitions are allowed to energy levels resulting from the combination of the two wag modes, which transform like the symmetrized product  $E_u \otimes E_g$ , or in terms of irreducible representations  $A_{1u} + A_{2u} + E_u$ . Hence, the line at  $1608\text{ cm}^{-1}$  could originate from the excitation of an  $E_u \otimes E_g$  combination level. The assignment of the lines to  $H_2^{**}$  may appear in contradiction with the results of the coimplantation experiments, where no additional lines associated with defects containing both H and D were observed. For the  $H_2^*$ , a small splitting is resolved for the  $H_{AB}$ - and  $H_{BC}$ -related stretch modes, but not for the wag mode of  $H_{AB}$ .<sup>12</sup> Since the distance between the two H atoms in  $H_2^{**}$  is substantially larger than for  $H_2^*$ , we expect the splitting between the mixed- and single-isotope stretch modes to be smaller,<sup>27</sup> due to a weak dynamical coupling between the two  $H_{AB}$  atoms. Keeping in mind the substantial width of the  $1306$  and  $1791\text{ cm}^{-1}$  lines, it appears likely that this splitting is too small to be resolved.

The stability and LVM frequencies for  $H_2^{**}$  have recently been calculated by *ab initio* theory.<sup>27</sup> It was found that the  $H_2^{**}$  structure represents a local minimum in energy for diatomic H in Si. The frequencies of the wag modes  $E_u$  and  $E_g$

are predicted at  $747$  and  $744\text{ cm}^{-1}$ , and the stretch modes  $A_{2u}$  and  $A_{1g}$  are found to be  $1824$  and  $1821\text{ cm}^{-1}$ . These values are in fair agreement with those observed and they confirm the weak dynamical coupling between the two H atoms.

## V. CONCLUSION

We have carried out *in situ*-type IR absorption measurements on proton-implanted Si. The IR spectra reveal three lines at  $812$ ,  $1608$ , and  $1791\text{ cm}^{-1}$ . Uniaxial stress measurements demonstrate that the defect giving rise to these lines has trigonal symmetry. Based on the analysis of the experimental data and on comparison with the properties of known H defects in Si, we assign the lines to the vibrations of  $H_{AB}$  attached to Si along a  $\langle 111 \rangle$  trigonal axis. We propose that the lines originate from  $H_2^{**}$  (shown in Fig. 1), but the positive charge state of a  $H_{AB}$  attached to a Si atom neighboring a vacancy cannot be ruled out completely.

## ACKNOWLEDGMENTS

We thank J. Coutinho for a number of valuable discussions and K. G. Bahner for assistance in running the accelerator. This work has been supported by the Danish Research Council for Natural Sciences and iNANO.

\*Electronic address: pereira@phys.au.dk; pereira@wsi.tum.de  
Present address: Walter Schottky Institute, Technical University Munich, 85748 Garching, Germany.

<sup>1</sup>*Hydrogen in Semiconductors*, edited by J. I. Pankove and N. M. Johnson (Academic, Boston, 1991), Semiconductors and Semimetals Vol. 34.

<sup>2</sup>*Hydrogen in Semiconductors II: Semiconductors and Semimetals*, edited by N. H. Nickel (Academic, New York, 1999), Vol. 61.

<sup>3</sup>S. J. Pearton, J. W. Corbett, and M. Stavola, *Hydrogen in Crystalline Semiconductors* (Springer-Verlag, Berlin, 1992).

<sup>4</sup>C. T. Sah, J. Y. C. Sun, and J. J. T. Tzou, *Appl. Phys. Lett.* **43**, 204 (1983).

<sup>5</sup>J. I. Pankove, D. E. Carlson, J. E. Berkeyheiser, and R. O. Wance, *Phys. Rev. Lett.* **51**, 2224 (1983).

<sup>6</sup>N. M. Johnson, C. Herring, and D. J. Chadi, *Phys. Rev. Lett.* **56**, 769 (1986).

<sup>7</sup>J.-F. Zheng and M. Stavola, *Phys. Rev. Lett.* **76**, 1154 (1996).

<sup>8</sup>Yu. V. Gorelkinskii and N. N. Nevinyi, *Physica B* **170**, 155 (1991), and references therein.

<sup>9</sup>B. Holm, K. Bonde Nielsen, and B. Bech Nielsen, *Phys. Rev. Lett.* **66**, 2360 (1991).

<sup>10</sup>K. B. Nielsen, B. B. Nielsen, J. Hansen, E. Andersen, and J. U. Andersen, *Phys. Rev. B* **60**, 1716 (1999).

<sup>11</sup>K. Bonde Nielsen, L. Dobaczewski, S. Søgård, and B. Bech Nielsen, *Phys. Rev. B* **65**, 075205 (2002).

<sup>12</sup>J. D. Holbeck, B. Bech Nielsen, R. Jones, P. Sitch, and S. Öberg, *Phys. Rev. Lett.* **71**, 875 (1993).

<sup>13</sup>M. Budde, B. Bech Nielsen, C. Parks Cheney, N. H. Tolk, and L. C. Feldman, *Phys. Rev. Lett.* **85**, 2965 (2000).

<sup>14</sup>M. Budde, Ph.D. Thesis, University of Aarhus, Denmark (1998).

<sup>15</sup>R. E. Pritchard, M. J. Ashwin, J. H. Tucker, R. C. Newman, E. C. Lightowers, M. J. Binns, S. A. McQuaid, and R. Falster, *Phys.*

*Rev. B* **56**, 13118 (1997).

<sup>16</sup>R. E. Pritchard, M. J. Ashwin, J. H. Tucker, and R. C. Newman, *Phys. Rev. B* **57**, R15048 (1998).

<sup>17</sup>A. W. R. Leitch, V. Alex, and J. Weber, *Phys. Rev. Lett.* **81**, 421 (1998).

<sup>18</sup>C. G. Van de Walle, Y. Bar-Yam, and S. T. Pantelides, *Phys. Rev. Lett.* **60**, 2761 (1988); C. G. Van de Walle, P. J. H. Denteneer, Y. Bar-Yam, and S. T. Pantelides, *Phys. Rev. B* **39**, 10791 (1989).

<sup>19</sup>K. J. Chang and D. J. Chadi, *Phys. Rev. Lett.* **62**, 937 (1989); *Phys. Rev. B* **40**, 11644 (1989).

<sup>20</sup>R. Jones, *Physica B* **170**, 181 (1991).

<sup>21</sup>S. K. Estreicher, M. A. Roberson, and D. M. Maric, *Phys. Rev. B* **50**, 17018 (1994).

<sup>22</sup>M. Budde, B. Bech Nielsen, R. Jones, J. Goss, and S. Öberg, *Phys. Rev. B* **54**, 5485 (1996).

<sup>23</sup>A. E. Hughes and W. A. Runciman, *Proc. Phys. Soc. London* **90**, 827 (1967).

<sup>24</sup>R. N. Pereira, B. B. Nielsen, A. R. Peaker, and N. V. Abrosimov, *Phys. Rev. B* **73**, 085201 (2006).

<sup>25</sup>A. Balsas, V. J. B. Torres, J. Coutinho, R. Jones, B. Hourahine, P. R. Briddon, and M. Barroso, *J. Phys.: Condens. Matter* **17**, S2155 (2005).

<sup>26</sup>E. B. Wilson, J. C. Decius, and P. C. Cross, *Molecular Vibrations: The Theory of Infrared and Raman Vibrational Spectra* (Dover, New York, 1980).

<sup>27</sup>J. Coutinho, V. J. B. Torres, R. N. Pereira, R. Jones, S. Öberg, and P. R. Briddon, *Mater. Sci. Eng., B* **124-125**, 363 (2005). In this paper, the LVMs for the H single-isotope configuration of  $H_2^{**}$  are predicted. Posterior calculations using the same theoretical method estimate frequency splittings between the mixed- and single-isotope stretch modes for the D- and H-related modes of  $0.6$  and  $2.1\text{ cm}^{-1}$ , respectively.